A Nonequilibrium Phase Diagram of the System HCl–H_2O Determined by ^1H NMR

Eddy Walther Hansen[†]

Department of Chemistry, University of Oslo, N-0315 Oslo 3, Norway

The proton chemical shifts of liquid hydrogen chloride solutions were measured against temperature and concentration and the data fitted to a polynomial in two variables by regression analysis. These liquid solutions were then frozen rapidly (high freezing rate) resulting in a nonequilibrium separation of solute between the two phases formed. By use of NMR the corresponding nonequilibrium phase diagram (solidus and liquidus) for the system HCl–H_2O was determined with a distribution coefficient that was strongly dependent on the initial dopant concentration. However, for dopant concentrations higher than 10^{-3} mole fraction, the distribution coefficient was found to be approximately constant and equal to 0.10. In comparison the distribution coefficient for equilibrium freezing, with convection, has been previously measured to be 2.7 × 10^{-3}.

Introduction

The question of a liquid phase in pure ice has been the subject of a number of investigations (*1–5*). The first direct observation of this phase was obtained by the nuclear magnetic resonance (NMR) technique (*3*, *5*). A narrow resonance line from highly mobile protons in pure ice was observed overlapping the much broader peak from the rigid ice protons. The same type of spectra is also observed in doped ice samples when the concentration of impurities is larger than the equilibrium concentration as determined from the corresponding phase diagram (*6*). A variety of simple aqueous solutions have been found to yield narrow proton resonances at subzero temperature (*7*), indicating that the NMR technique affords a quick and convenient method for the construction of equilibrium phase diagrams (*6*). However, freezing often takes place under nonequilibrium conditions, that is, when the freezing rate is fast relative to the diffusion rate of the solute in the solution. An excess amount of solute molecules will then be trapped in the solid phase. In this paper, the properties and phase diagram of such a nonequilibrium system will be reported. The HCl–H_2O system studied in this work was chosen primarily because its first eutectic point appears at a relatively low temperature of approximately −74 °C. The correspondingly broad temperature range (from 0 °C to −74 °C) makes this system fairly suitable for an experimental study. In addition, the spin–lattice relaxation time (T_1) of the solid phase in ice doped with a selection of acids (HCl among others), salts, and bases has quite recently been the subject of an intensive NMR study (*8*). The results presented in this work will give additional information concerning the distribution of dopant (HCl) molecules between the solid and liquid phase, respectively.

Experimental Section

A. Sample Preparation. Samples of ice doped with HCl were prepared from a concentrated purum quality (>99% Fluka) solution of HCl which was diluted to different concentration levels: 2 × 10^{-5}, 5 × 10^{-5}, 8 × 10^{-5}, 1 × 10^{-4}, 5 × 10^{-4}, 1 × 10^{-3}, 4 × 10^{-3}, 10^{-2}, 2.4 × 10^{-2}, 4.1 × 10^{-2}, 6.7 × 10^{-2}, 8.4 × 10^{-2}, 0.1, 0.12, 0.137 mole fraction. These solutions were filled in NMR tubes (diameter 5 mm, wall thickness 0.4 mm), quenched in liquid nitrogen, and then stored at −96 °C for at least 24 h before measurements were performed.

B. Apparatus and Measuring Technique. The proton spectra were obtained on a Bruker CXP-200 pulse FT NMR spectrometer. Nine hundred scans were accumulated for the lowest dopant concentration studied (2 × 10^{-5}) using a bandwith of 2 kHz with 16K data points giving a digital resolution of 0.246 Hz. For the highest dopant concentration only 16 scans were accumulated. The pulse angle was set to approximately 22° while the waiting time between pulses was adjusted in order to ensure that the equilibrium magnetization of the TMS signal was attained (9 s at 0 °C and 3 s at −70 °C, see ref *9*). The necessity of taking into account the spin–lattice relaxation time of the TMS peak has to do with the quantitative aspect of the measurements and will be explained later.

All the NMR spectra determined in this work have been analyzed by a curve-fitting procedure in order to minimize the uncertainty in the line-width and chemical shift measurements (*10*). The intensity (area) of the NMR peaks were measured by applying an integration procedure described by Chan and Commisarov (*11*). The temperature was measured with a so-called "NMR thermometer" placed in a capillary inside the ice sample (*12*). In this way a temperature spectrum and a sample spectrum were recorded simultaneously, and the temperature was determined with an accuracy of 0.7 °C and remained stable to within 1 °C during the measurement. This same capillary also contained 6% by volume of TMS to be used as an external chemical shift reference.

C. Determination of the Normalized Liquid-Phase Intensity. Measurement of the liquid signal intensity at any temperature below the freezing point is generally normalized by comparison with the intensity of the same sample when melted. However, this procedure might introduce serious errors because of changes in sensitivity of the electromagnetic characteristics of the rf coil assembly with a change in temperature, sample, or sample form. Secondly one should keep in mind the proportionality between magnetization and the reciprocal of the absolute temperature (*13*). However, all of these serious limitations can be circumvented by taking into account the intensity of the TMS peak (from the NMR thermometer). The "true" normalized liquid intensity (f) can thereby be estimated from

$$f = \frac{I_l}{I_{TMS}} \frac{I_{TMS}^0}{I_l^0} \quad (1)$$

where I_l is the intensity (area of NMR absorption signal) of the proton signal from the liquid phase, I_{TMS} is the intensity of the proton signal from TMS in the capillary, I_l^0 is the intensity of the total proton signal at t = 0 °C (measured by melting the sample after having completed all other measurements, and I_{TMS}^0 is the intensity of the proton signal from the TMS peak at t = 0 °C. In order to record spectra containing quantitative information, the time interval between pulses must be at least 3 times the longer T_1 of the two components, liquid sample, and TMS (*14*). In this study TMS has the longer T_1 and therefore

[†] Permanent address: Production Laboratories, Statoil, P.O. Box 300, Forus, N-4001 Stavanger, Norway.

0021-9568/88/1733-0099$01.50/0

determines the experimental parameter setting.

Results and Discussion

Preliminary. Freezing Point Diagram of the System HCl–H_2O. This diagram was first determined by Pickering (*15*) and later Roloff (*16*) who found the coordinates of the first eutecticum at −87.5 °C and 24.8 mass % of hydrogen chloride. In 1955 Vuillard (*17*) showed that this eutecticum in fact was a metastable eutecticum. By first quenching the sample in liquid nitrogen and then keeping it at −96 °C for at least 24 h he was able to determine the eutectic point to be −74.7 °C and 23.0 mass % of hydrogen chloride. However, the freezing point curve determined by these authors do not reveal any significant mutual differences and we have therefore used all available temperature and concentration data (*15–17*) in order to construct an analytical expression between the two parameters. On a rather intuitive basis we have used the formula given by eq 2 for this fitting procedure. (Note the similarity between this expression and the well-known Clausius–Clapeyron equation).

$$\frac{d}{dT} \ln (1 - \phi C_l) = \frac{\Delta H_{TMS}}{RT^2} \qquad (2)$$

In eq 2 H is the molar heat of fusion of pure water, T is the absolute temperature, and C_l is the concentration of solute in the liquid phase expressed in mole fraction of solute in the solution. The parameter ϕ might be looked upon as some kind of an "activity coefficient". However, no physical weight is given to this fitted parameter but eq 2 is simply regarded as a convenient way of presenting the available literature data. ϕ was approximated by a polynomial given by

$$\phi = B_0 + B_1 T + B_2 T^2 \qquad (2a)$$

where $B_0 = -9.0963$, $B_1 = 0.15368$, and $B_2 = -4.1745 \times 10^{-4}$. The standard error of estimate between the observed and calculated temperatures (eq 2) was 0.45 °C and reflects mainly the inherent spread in the experimental data. Equation 2 is used repeatedly throughout this work.

Chemical Shift of Liquid HCl Solutions versus Temperature and Concentration. A detailed analysis of the behavior of the chemical shift versus temperature and concentration of liquid hydrogen chloride solutions has been investigated. Eight different concentrations ranging from 0.0243 (freezing point equal to −5.4 °C) and up to 0.1397 mole fraction (freezing point equal to −87.4 °C) have been studied. Before any measurement was carried out, the system was allowed to temperature equilibrate for 10 min after a temperature change while the sample was continually spun with a rate of 20 cps throughout the experiment. The liquid solutions studied were all observed to be supercooled far below their expected freezing point, at least 5–10 deg for the lower concentrations and up to 15 deg for the higher concentrations.

The observed chemical shift (δ) were fitted to a polynomial in two variables, temperature (T) and concentration (C), using 160 data points and utilizing the method of least squares.

$$\delta = (A_1 + A_4 C + A_5 C^2) + (A_2 + A_6 C + A_8 C^2) T + (A_3 + A_7 C + A_9 C^2) T^2 \qquad (3)$$

where $A_1 = 1.0896 \times 10^1$, $A_2 = -3.3836 \times 10^{-2}$, $A_3 = 3.6869 \times 10^{-5}$, $A_4 = -4.1680 \times 10^1$, $A_5 = 1.3554 \times 10^2$, $A_6 = 3.2484 \times 10^{-1}$, $A_7 = -4.4181 \times 10^{-4}$, $A_8 = -8.1046 \times 10^{-1}$, and $A_9 = 1.0997 \times 10^{-3}$. The standard deviation in the chemical shift (δ) was measured to be 0.0025 ppm. It has to be emphasized that in these measurements only a liquid phase was present and no solid was formed. Recall that the chemical shift values have not been corrected for susceptibilities. However, this effect is of no concern to this work. By combining eq 2 and eq 3 the chemical shifts of hydrogen chloride solutions at their respective freezing points were determined. The results are shown by the solid curve in Figure 2C and Figure 3.

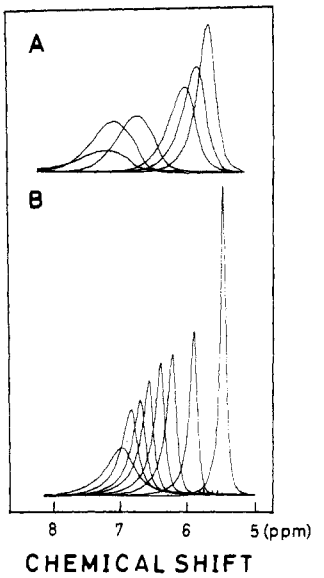

Figure 1. Some of the experimental NMR spectra of the liquid phase in HCl-doped ice (0.040 89 mole fraction) versus temperature (see also Figure 2). (A) First annealing cycle, temperatures from left to right −74, −65.1, −49.8, −24.8, −20.4, and −16.5 °C. (B) Subsequent cooling cycle, temperatures from right to left −22.8, −38.5, −53.6, −63.1, −74.6, −83.8, −94.0, and −103 °C.

Nonequilibrium Phase Diagram of the System HCl–H_2O. Some experimental NMR spectra showing the behavior of the line width (ΔB), chemical shift (δ), and intensity (f) of the liquid phase versus temperature for the 0.040 89 mole fraction HCl–H_2O solution are presented in Figure 1 and the numerical data plotted in Figure 2. The same characteristics are found for all the other hydrogen chloride solutions as well. The following discussion will therefore be limited to the results presented in Figure 2.

When a liquid hydrogen chloride solution was frozen according to the procedure of Vuillard (*17*) and then annealed slowly from −96 °C, a liquid phase appeared at first above −74 °C (black dots in Figure 2) which is in agreement with earlier measurements (*17*). A further increase in temperature resulted in a monotonic decrease in line width and chemical shift but an increase in the signal intensity because more liquid was being formed. When the sample was close to its melting point the temperature change was reversed and a cooling of the system was started (open circles in Figure 2). A marked change could now be observed in the chemical shift and line width compared to the earlier annealing curve, indicating that an irreversible change was taking place. However, the intensity of the liquid signal remained unchanged (to within experimental error). During a second annealing cycle no observable changes in the three NMR parameters versus temperature could be detected compared to the last cooling cycle, so that a reversible state of the system had been attained (these data points are only illustrated by an arrow in Figure 2 and not plotted because they coincide with the previous cooling curve). This means that for a given temperature the experimental NMR parameters—for instance, the chemical shift—will be the same independent of the previous temperature history of the sample. During the cooling of the sample, after the first annealing period, the signal did not disappear at −74 °C, indicating that the system had entered the metastable state with a predicted eutecticum of −87 °C (*15–17*). However, the liquid phase in all the samples studied in this work remained liquid far below −87 °C. Even at a temperature of −103 °C a liquid phase was still detectable, demonstrating the existence of a substantially supercooled liquid phase. The temperature was not reduced any further because of practical limitations with the cooling unit and problems with

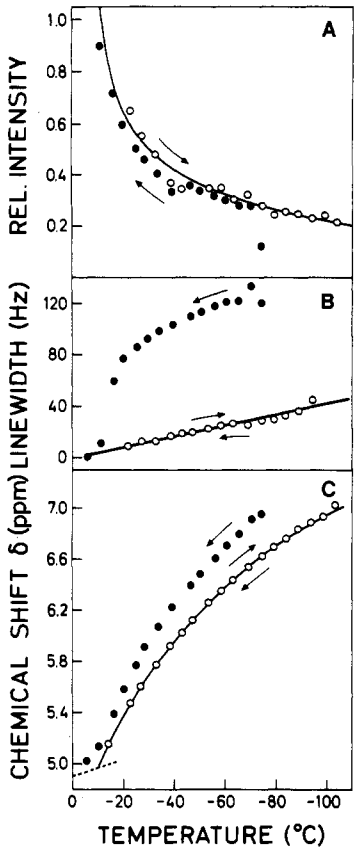

Figure 2. (A) Normalized intensity of the liquid-phase NMR signal in HCl-doped ice versus temperature. (B) Line width at half-height of the liquid-phase NMR signal in HCl-doped ice versus temperature. (C) Chemical shift of the liquid-phase NMR signal in HCl-doped ice versus temperature. The open circles (O) represent the first annealing cycle while the black dots (●) represent the subsequent cooling of the sample. The arrows indicate the direction of temperature change. Note the reversible change in the NMR parameters after the first annealing (C_0 = 0.040 89 mole fraction).

the freezing of the NMR thermometer.

A hydrogen chloride solution of concentration C_0 and a corresponding freezing point T_0 is seen to have the same chemical shift as a liquid phase coexisting with a solid phase at the same temperature (T_0). This is illustrated in Figure 3 from which we conclude that the chemical shift of the liquid phase is unaffected by the simultaneous presence of a solid phase. It might well be, however, that the solute molecules in the solid and the liquid phase constitute a nonequilibrium distribution.

All the results presented in the subsequent discussion have been taken from the first cooling curve in order to ensure the equilibrium freezing diagram (eq 2) to be applicable to the liquid phase in the ice sample. Before proceeding further a few additional comments will be given on the results presented in Figure 2.

The big difference in the chemical shift of the liquid phase between the first (black dots) and the second (open circles) annealing cycle (at a given temperature) indicates a corresponding difference in the HCl concentration. This conclusion is based on the additional observation that the liquid intensity of the two annealing cycles remains the same. However, Figure 2B reveals a dramatic change in line width between the same two annealing cycles which brings about another possible explanation that can be traced back to a susceptibility effect. This means that the observed differences in chemical shift between the two annealing cycles are not real but related to the fact that they (chemical shift) are not corrected for susceptibility.

Irrespective of these observations, the liquid phase after the first annealing cycle can be looked upon as an isolated phase

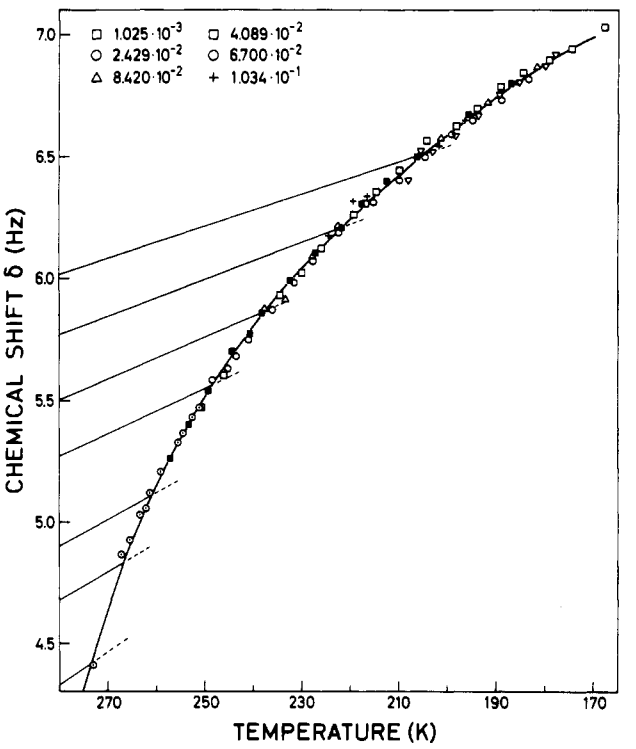

Figure 3. Chemical shift of the liquid phase in HCl-doped ice versus temperature and initial dopant concentration (mole fraction). The solid curve through the points is calculated from the "equilibrium freezing point curve". The almost parallel lines to the left of the figure represent the chemical shift of the liquid solutions when no solid solution is formed. The corresponding concentrations of these "parallel lines" are from bottom to top 1.025 × 10^{-3}, 2.429 × 10^{-2}, 4.089 × 10^{-2}, 6.717 × 10^{-2}, 8.415 × 10^{-2}, 1.025 × 10^{-1}, and 1.215 × 10^{-1}.

in thermodynamic equilibrium with a concentration given by eq 2.

Another possible explanation of the data presented in Figure 2 might be that a rather inhomogeneous distribution of dopant molecules throughout the ice sample is generated after the rapid freezing but that this distribution becomes more homogeneous after an additional annealing cycle. This explanation is more questionable because rapid freezing should automatically lead to a more homogeneous distribution.

A more complete discussion on these effects will be reported elsewhere.

Solidus. In a two-phase, two-component system the average concentration of dopant in each phase is given by the "lever rule", which may be written

$$C_0 = (1 - f_l)C_s + f_l C_l \quad (4)$$

where f_l is the number of H_2O molecules in the liquid phase/total number of H_2O molecules in the sample; C_l is the number of HCl molecules in the liquid phase/number of H_2O molecules in the liquid phase; C_s is the number of HCl molecules in the solid phase/number of H_2O molecules in the solid phase; and C_0 is the total number of HCl molecules in the sample/total number of H_2O molecules in the sample. Equation 4 expresses a mass balance which is valid both under equilibrium and nonequilibrium conditions.

To obtain the phase diagram of the system, the three parameters C_l, C_s, and f_l have to be measured as a function of temperature. We have done this in the following way.

Measurement of f_l. The parameter f_l is obtained from measurement of the normalized intensity (f) of the proton NMR signal (Figure 4) by the use of the equation

$$f_l = \frac{2 + C_0}{2 + C_l} f \quad (5)$$

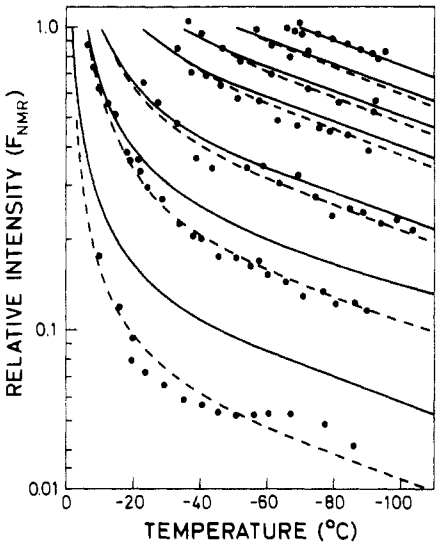

Figure 4. NMR intensity (normalized) of the liquid-phase signal of doped ice versus temperature and initial dopant concentration C_0. The C_0 concentrations are from bottom to top in mole fraction 0.001, 0.024 29, 0.040 89, 0.067 17, 0.081 15, 0.1025, and 0.1215. (The 0.001 mole fraction is displayed in the bottom part and is displaced by a factor of 10 from its real value.) The solid curves are calculated from the assumption that no dopant molecules enter the solid phase. The dotted lines are calculated from eq 5 by using the C_s values shown in Figure 4. The curves calculated by assuming the C_s values to be independent of temperature (constant) coincide with these previous curves (dotted).

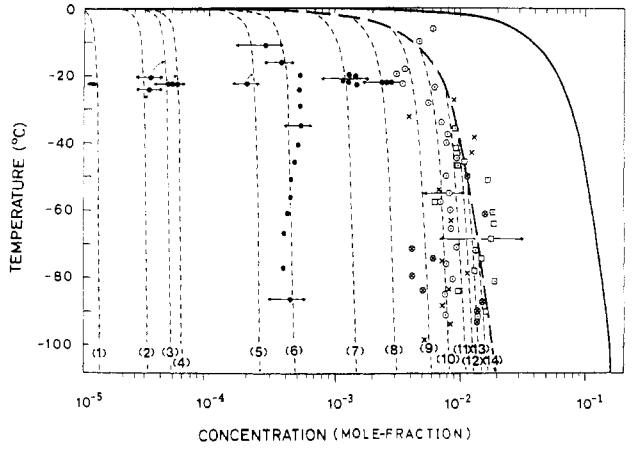

Figure 5. Nonequilibrium phase diagram of the system HCl–H_2O showing both the liquidus (—) and the solidus (– – –). The latter depends on the initial concentration of HCl as given by (1) 2×10^{-5}, (2) 5×10^{-5}, (3) 5×10^{-5}, (4) 1×10^{-4}, (5) 5×10^{-4}, (6) 1×10^{-3}, (7) 4×10^{-3}, (8) 1×10^{-2}, (9) 2.4×10^{-2}, ⊙; (10) 4.1×10^{-2}, ×; (11) 6.7×10^{-2}, ⊡; (12) 8.4×10^{-2}, □; (13) 0.1, ⊗; (14) 0.1215. The thick dashed line (—) represents the solute concentration in the solid at the advancing solid front.

Measurement of the Liquidus C_l. C_l is, as already noted, calculated from the equilibrium or freezing point curve, eq 2, with ϕ given by eq 2a.

Measurement of the Solidus C_s. C_s is determined from the lever rule (eq 4) and plotted in Figure 5. By rearrangement of this equation, a simple calculation shows that the uncertainty in C_s is increasing with a corresponding increase in f_l. This effect can come about by either an increase in temperature and/or an increase in the initial concentration C_0.

The equilibrium solubility of HCl in ice has been determined by Krishnan and Salomon (*18*) to be at mole fraction of 1.4×10^{-7} at −10 °C. Figures 5 and 6 in this work demonstrate a much higher concentration of HCl in the solid phase and moreover this concentration is strongly dependent on the initial dopant concentration C_0. In spite of the faster freezing rate applied to these solutions, a solubility limit seems to exist at a

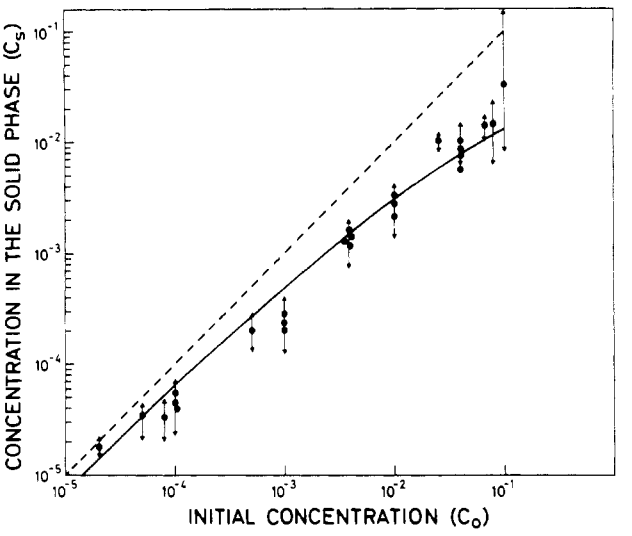

Figure 6. Experimental values of the solid-phase concentration (C_s) versus initial dopant concentration C_0 at −74 °C. The solid curve is calculated as described in the text while the dotted line represents a situation where no dopant molecules enter the liquid phase.

concentration given by approximately 0.015 mole fraction at −74 °C. A nonequilibrium state between the two coexisting phases is thereby formed. Since the diffusion rate of HCl in ice (4×10^{-7} cm^2/s) is extremely small (*8*) compared to times involved in the experiment, by supposing the transport of HCl between the two phases to be negligible, the existence of a quasi-equilibrium state can be assumed. With this in mind a very general relation (eq 6) can be obtained between (1) the solute concentration C in the solid at the advancing solid front, (2) the solute concentration C_l in the liquid phase adjacent to the solid freezing front, and (3) the total fraction melted f_l. This equation is obtained by means of a simple mass balance consideration (*19*)

$$\ln f_l = \int_{C_0}^{C_l} \frac{dC_l}{C - C_l} \tag{6}$$

Since the position of the liquidus and thus C_l is known at any temperature, and since the fraction melted, f_l, has been measured by NMR, the solute concentration (C) in the solid at the advancing solid front (i.e., C as a function of temperature) can be found by integration of eq 6. We follow the same procedure as proposed by Herington and Lawrenson (*20*) and assume that C can be expressed as a function of C_l given by

$$C = C_l + \frac{1}{\frac{a_{-2}}{C_l^2} + \frac{a_{-1}}{C_l} + a_0 + a_1 C_l + a_2 C_l^2 + \dots} \tag{7}$$

Then

$$\ln f_l = -a_{-2}\left(\frac{1}{C_l} - \frac{1}{C_0}\right) + a_{-1} \ln \frac{C_l}{C_0} + a_0(C_l - C_0) + \frac{1}{2}a_1(C_l^2 - C_0^2) + \frac{1}{3}a_2(C_l^3 - C_0^3) + \dots \tag{8}$$

The 118 experimental data points (C_l, C_0, f_l) were fitted to eq 8 in order to determine the coefficients a_i. The least number of coefficients needed was 2 and the relative standard deviation in f_l was estimated to be 13.5% which mainly reflects the relative uncertainty in each f_l measurement of approximately 10%. The values found for a_{-2} and a_{-1} were $a_{-2} = -2.398 \times 10^{-5}$ and $a_{-1} = -1.106$. In order to calculate the solidus C_s for any initial concentration C_0 and at any temperature, the lever rule (eq 4) was combined with eq 8 (f_l values) and eq 2

Table I. Freezing Points Determined from Chemical Shift and Intensity Measurements of HCl-Doped Ice[a]

C_0	T_0, °C	T_0^δ, °C	T_0^t, °C	C_0^t, °C	$\bar{C}_s$
1.025×10^{-3}	−0.2	−0.0 ± 0.5	−0.8 ± 0.6	(1.035 ± 0.148) × 10^{-3}	4.41×10^{-4}
2.429×10^{-2}	−5.4	6.7 ± 0.7	−5.5 ± 0.7	(2.472 ± 0.250) × 10^{-2}	5.03×10^{-3}
4.089×10^{-2}	−10.6	−12.5 ± 0.9	−11.3 ± 1.2	(4.265 ± 0.320) × 10^{-2}	7.38×10^{-3}
6.717×10^{-2}	−23.2	−24.7 ± 1.4	−22.9 ± 1.7	(6.700 ± 0.240) × 10^{-2}	1.01×10^{-2}
8.415×10^{-2}	−35.0	−35.5 ± 2.0	−36.2 ± 3.1	(8.570 ± 0.370) × 10^{-2}	1.18×10^{-2}
1.025×10^{-1}	−51.0	−50.5 ± 2.6	−51.9 ± 4.2	(1.034 ± 0.440) × 10^{-1}	1.19×10^{-2}
1.215×10^{-1}	−69.4	−68.4 ± 2.9	−69.4 ± 3.9	(1.215 ± 0.410) × 10^{-1}	1.57×10^{-2}

[a] C_0 is the initial concentration, prior to freezing, determined by titration; T_0, freezing point determined from eq 2 with a RMS error of 0.5 °C; T_0^t, freezing point determined from intensities (see (Liquidus, section C); T_0^δ, freezing point determined from chemical shift (see Liquidus, section A); C_0^t, initial concentration determined from intensity measurements (see Liquidus, section C); $\bar{C}_s$, calculated average concentration of HCl in the solid phase at −74 °C at the indicated initial concentration C_0.

(C_l values). The results of these calculations are plotted in Figure 5 (dashed lines) together with the solute concentration (C) in the solid at the advancing solid front (eq 7). The "observed" C_s values at −74 °C are plotted in Figure 6 together with the values calculated by the preceding model (solid line). The uncertainties illustrated in this same figure are estimated from eq 4 by assuming the error in C_0 and C_l to be negligible. The mole fraction of HCl in the solid ice sample was measured to be approximately 80 ± 10% for the lowest initial dopant concentration studied $C_0 = 2 \times 10^{-5}$ and decreasing to 25 ± 10% for $C_0 = 1 \times 10^{-3}$ (Figure 6). The calculated monotonic increase of the solidus (Figure 5) versus temperature was too small to be observed experimentally by NMR. This will be discussed in the next section.

Liquidus. The equilibrium phase diagram has already been shown to be useful in describing the liquid phase of the nonequilibrium HCl–H_2O system. This liquidus, tie line, or freezing point curve might be determined by NMR in three different ways as indicated by the results presented in Figure 2.

A. It is an experimental observation that the chemical shift of the liquid phase versus temperature $\delta(T)$ to have a discontinuity in its first derivatives $\delta'(T)$ at the freezing point. This is illustrated by the data points given in Figure 2C where the solid and dotted lines represent the chemical shift of the liquid phase below and above the melting point, respectively. Additional data are plotted in Figure 3 where the effect of a change in concentration is shown. By fitting the two lines by a second-order polynomial and determining the point of intersection between them an approximate value of the freezing point was determined. The results of these calculations are given in Table I together with the estimated uncertainties. One has to bear in mind that the absolute uncertainty in the freezing point determined in this way is increasing with a corresponding increase in concentration of dopant. This statement is best illustrated by the fact that the derivative of the chemical shift versus temperature along the liquidus is decreasing with a decrease in temperature (Figure 3).

B. Another way of approximating the melting point is to plot the line width versus temperature and to determine, by extrapolation, the temperature at zero line width. This procedure has been applied to the data shown in Figure 2B (open circles) by assuming a straight line to exist between temperature and line width. The value found for the freezing point with this procedure was −4.8 °C compared with the true melting point of −10.6 °C. This discrepancy might be due to the fact that the linear model chosen is too crude. Unfortunately, no theoretical model is available in describing the temperature behavior of the line width of a liquid phase coexisting with a solid phase. On this background a further discussion on this subject will not be presented in this work.

C. The last technique applied in determining the freezing point will be discussed in more detail. The solute concentration (C) in the solid at the advancing solid front of the system HCl–H_2O has been determined by use of eq 7. In so doing the solidus C_s (C_0, T) was calculated at any temperature and any initial dopant concentration as described earlier in the section Measurement of the Solidus C_s.

The experimental NMR intensities (f_i) measured for different dopant concentrations (C_0) and different temperatures (T_i) are shown in Figure 4. Let us draw attention to those points belonging to a given C_0 concentration and assume that this concentration C_0 itself is unknown. By making a guess at the value of C_0 we can calculate the concentration C_s' in the solid phase at the temperature T_i from the previous equation $C_s(C_0,T)$ and at the same time determine the concentration $C_l(T_i)$ in the liquid phase from eq 2. By rearranging eq 4 and applying eq 5 we end up with an estimated value of f_i denoted by f'_{calcd}. By changing the input parameter C_0 we repeat the whole calculation until the expression $\sum(f_i - f'_{calcd})^2$ reaches a minimum. The value of C_0 so determined is given in Table I and the corresponding expression for f (eq 4) is plotted in Figure 4 (dotted line) together with the results found if no dopant molecules entered the solid phase, that is, $C_s = 0$ (solid line).

The freezing point of the solution is then determined be setting $f = 1$. Results are given in Table I. The two set of curves displayed in Figure 6 (solid and dotted) for each initial concentration C_0 shows clearly that there is an increasing relative amount of dopants in the solid phase with a decrease in C_0. If we, instead of the small monotonic increase in C_s versus temperature, as determined previously (dotted curve in Figure 5), rather assume the C_s to be constant throughout the temperature range and equal to its temperature average ($\bar{C}_s$ in Table I), then no significant change in the calculated f values could be determined. In short, in light of these NMR experiments no observable inhomogeneities in the solid phase could be detected.

The last comment on this dopant system will deal with the equilibrium distribution coefficient $k = C/C_l$ as determined by Gross et al. (*21*) when spontaneous convection in the liquid phase was applied. They measured a value of k equal to 2.7 × 10^{-3} and found that it was independent of the initial dopant concentration.

Equation 7, presented in this work, can be simplified and recast in the form

$$k = \frac{C}{C_l} = 1 + \frac{1}{\frac{a_{-2}}{C_l} + a_{-1}} \qquad (9)$$

When $C_l > 10^{-3}$ eq 9 can be approximated by

$$k = 1 + (1/a_{-1}) \cong 0.10$$

which shows that k is independent on the initial dopant concentration C_0 but that the distribution coefficient is much higher than the one found by Gross et al. (*21*). This observation is simply a confirmation of the rapid and thereby nonequilibrium freezing rate applied to the liquid samples studied in this work.

We see that the k value is strongly dependent on the liquid-phase concentration C_l when $C_l < 10^{-4}$ mole fraction. Note also that k approaches the value 1 when $C_l \to 0$. However,

no liquid phase was observed when $C_0 < 10^{-6}$ mole fraction.

Acknowledgment

I am grateful to Prof. Bjørn Pedersen, Department of Chemistry, University of Oslo, and to Dr. Dag Slotfeldt-Ellingsen, Senter for Industriforskning (Oslo), for their valuable suggestions and support in the preparation of this manuscript.

Registry No. HCl, 7647-01-0.

Literature Cited

(1) Fletcher, N. H. *Philos. Mag.* **1962**, *7*, 255-268.
(2) Jillinke, H. H. G. *J. Appl. Phys.* **1981**, *32*, 1793.
(3) Akitt, J. W.; Lilley, T. H. *Chem. Commun.* **1967**, 323.
(4) Kvlividze, V. I.; Kiseley, V. F.; Kuzaev, A. B. *Surf. Sci.* **1974**, *44*, 6068.
(5) Clifford, J. *Chem. Commun.* **1967**, 880.
(6) Derbyshire, W. In *Water a Comprehensive Treatise*; Franks, F., Ed.; Plenum: New York, 1982; Vol. 7, Chapter 4.
(7) Ramirez, J. E.; Cavanaugh, J. R.; Purcell, J. M. *J. Phys. Chem.* **1974**, *78*, 807-810.
(8) Barnaal, D.; Slotfeldt-Ellingsen, D. *J. Phys. Chem.* **1983**, *87*, 4321-4325.
(9) Kessler, V. D.; Waiss, A.; Witte, H. *Ber. Bunsen-Ges. Phys. Chem.* **1967**, *71*, 3-19.
(10) Weiss, G. H.; Ferretti, J. A.; Kiefer, J. E. *J. Magn. Reson.* **1982**, *46*, 69-83.
(11) Chan, A.; Commisarov, H. *J. Magn. Reson.* **1983**, *51*, 252-263.
(12) Hansen, E. W. *J. Anal. Chem.* **1985**, *57*, 2993.
(13) Abragam, A. *The Principles of Nuclear Magnetic Magnetism*; Clarendon: Oxford, U.K., 1961.
(14) Abraham, R. J.; Loftus, P. *Proton and Carbon-13 NMR Spectroscopy. An Integrated Approach*; Heyden: London, 1968; p 123.
(15) Pickering, S. U. *Ber. Dtsch. Chem. Ges.* **1883**, *26*, 277-284.
(16) Roloff, Z. *Phys. Ch.* **1895**, *18*, 576.
(17) Vuillard, G. *C. R. Acad. Sci.* **1955**, *241*, 1308-1311.
(18) Krishnan, P. N.; Salomon, R. E. *J. Phys. Chem.* **1969**, *73*, 2680.
(19) Herington, E. F. G. In *Zone Refining of Organic Compounds*; Blackwell: Oxford, U.K., 1963.
(20) Herington, E. F. G.; Lawrenson, I. J. *J. Appl. Chem.* **1969**, *19*, 341-344.
(21) Gross, G. W.; Pui Mun Wong; Humas, K. *J. Chem. Phys.* **1977**, *11*, 5264-5273.

Received for review October 1, 1986. Accepted August 10, 1987.

Thermodynamic Properties of Binary Acid–Base Mixtures

M. C. S. Subha and S. Brahmaji Rao*

Department of Chemistry, Sri Krishnadevaraya University, Anantapur 515 003 India

Densities and viscosities at 308.15 K were determined for the systems propionic acid (PA) + aniline (A), + *N*-methylaniline (MA), and + *N*-ethylaniline (EA). From the experimental results, the excess molar volumes, excess viscosities, and excess molar free energy of activation of flow were calculated. The results are discussed in terms of theories of nonelectrolyte solutions. Deviations from ideal behavior are more pronounced for the system PA + A than for the systems PA + MA and PA + EA. The results suggest complex formation between the components in all the systems in the mole ratio 2:1 (PA:anilines) approximately.

Very few studies (*1-3*) on properties such as viscosities, densities, and refractive indices of nonelectrolyte acid–base binary liquid mixtures have been reported. We have therefore taken up such studies as a continuation of our studies (*4*, *5*) on properties of nonelectrolytes.

The results obtained for the systems propionic acid (PA) + aniline (A), + *N*-methylaniline (MA), and + *N*-ethylaniline (EA) are reported in this paper.

Densities and viscosities of the systems mentioned were measured at 308.15 K. Excess functions V^E (excess molar volume), η^E (excess viscosity), and G^{*E} (excess molar free energy of activation of flow) were calculated from the experimental results at different mole fractions. The values obtained are discussed in terms of nonelectrolytic interactions.

Experimental Section

Densities were measured with a 18-mL bicapillary pycnometer having a capillary diameter of 0.85 mm. The pycnometer was calibrated by using double distilled water (density 994.06 kg m^{-3} at 308.15 K). All weighings were done on a Mettler balance (±0.05 mg). The necessary buoyancy correction was applied. The density values were reproducible within ±0.2 kg m^{-3}. A thermostatically controlled water bath, capable of maintaining the temperature constant to ±0.02 K, was used in the studies.

Table I. Physical Properties of the Liquids Investigated at 308.15 K

liquid	density, kg m^{-3}		viscosity, kg m^{-1} s^{-1} × 10^4	
	this work	lit.[a]	this work	lit.[a]
propionic acid	978.2	978.0	8.894	8.885
aniline	1008.8	1008.9	26.153	26.630
N-methylaniline	973.9	973.6	15.146	15.470
N-ethylaniline	948.5	948.4	14.999	15.490

[a] Reference 7.

Viscosities of the pure liquids and the liquid mixtures were detd. with a modified Ostwald viscometer. The time of efflux of a constant volume of liquid through the capillary was measured with the help of a precalibrated ROCAR stop watch capable of recording ±0.1 s. The viscometer was always kept in a vertical position in a water thermostat at 308.15 ± 0.02 K. The efflux time for water at 308.15 K was about 302 s. The flow time was maintained at deliberately high value to minimize the kinetic energy corrections.

The viscosity was calculated from the average efflux time, t, and density, ρ, according to

$$\eta/\rho = at - b/t \quad (1)$$

where a and b are the characteristic constants of the viscometer. The constants were determined by taking water and benzene as the calibrating liquids and used to calculate the kinetic energy correction. The corrections were found to be negligible. The viscosity measurements were accurate to ±0.5 × 10^{-4} kg m^{-1} s^{-1}.

Propionic acid (from Fluka, puriss grade, purity ≫ 99 mol % $C_2H_5CO_2H$) was dried over anhydrous sodium sulfate and fractionally distilled. The fraction distilling at 412.15–415.15 K was

0021-9568/88/1733-0104$01.50/0